Transplantation of *Macaca cynomolgus* iPS-derived hematopoietic cells in NSG immunodeficient mice

The use of iPSCs to generate hematopoietic stem/progenitor cells (HSPC) is of considerable therapeutic interest, as allogeneic HSPC transplantation is limited by the lack of compatible donors, a high risk of engraftment failure and GVHD. Efficacy and safety assessments are required and non-human primates (NHP) are the most appropriate animal model for preclinical validation. We generated and characterized *Macaca cynomolgus* iPSCs (cy-iPSCs). We assessed their capacity to differentiate *in vitro*, in the presence of hematopoietic cytokines, and determined the molecular signature triggered during hematopoietic differentiation. We then investigated cy-iPSC-derived hematopoietic cell engraftment in NSG mice, an essential step before the scaling up of hematopoietic cell production for autologous transplantation in monkeys.

Cynomolgus primary cells were refractory to standard reprogramming techniques.[1] However, we were able to reprogram them efficiently through two rounds of retroviral transduction with molecules known to improve iPSC generation (a mixture of SB431542, PD0325901, and thiazovivin, or VPA alone),[2] using the procedure summarized in the *Online Supplementary Figure S1*. Cy-iPSCs expressed the pluripotency marker alkaline phosphatase, SSEA4 and the endogenous factors NANOG, REX-1, OCT3/4, SOX2, KLF4 and MYC. Several iPS clones displayed incomplete silencing of the exogenous genes, although all expressed the *DNMT* genes involved in the de novo methylation of proviral DNA,[3] consistent with previous reports[4] and with the known incomplete silencing of the MSCV-derived vectors used here[5] (*Online Supplementary Figure S2A-D,F*). The teratomas developing from cy-iPSCs contained tissues originating from the three germ layers. DNA methylation studies showed the OCT3/4 and NANOG promoters to be less methylated in cy-iPSCs than in primary cells, which is consistent with transcriptional activation. Cytogenetic analysis revealed a normal female karyotype (42,XX) (*Online Supplementary Figure S2E,G,H*).

We investigated the hematopoietic potential of three clones in an embryoid body (EB) differentiation strategy. They all produced hematopoietic cells with similar efficiencies, despite the absence of exogenous gene silencing. Data are presented for cy-iPSC-cl29, which had the lowest spontaneous differentiation rate during iPSC expansion. At around day 15, EBs formed transparent sac-like structures containing bright round cells, which spilled into the supernatant over the course of several days and were able to form hematopoietic colonies. We performed FACS on cells obtained from EBs and supernatants (Figure 1B-A,C). On day 4, the EBs contained 5% $CD34^+$ cells. This proportion increased to 15% on day 8, and 2-3% of these cells were $CD34^+CD31^+CD45^-$. As for hESCs,[6] the hematopoietic marker CD45 was not detected prior to day 10, and its expression level increased over time, reaching 8% by day 21. CD11b myeloid cells were detected on day 10 and accounted for 5% of cells on day 21 (Figure 1A). Only a few cells could be retrieved from the supernatant before day 14 and were used for colony-

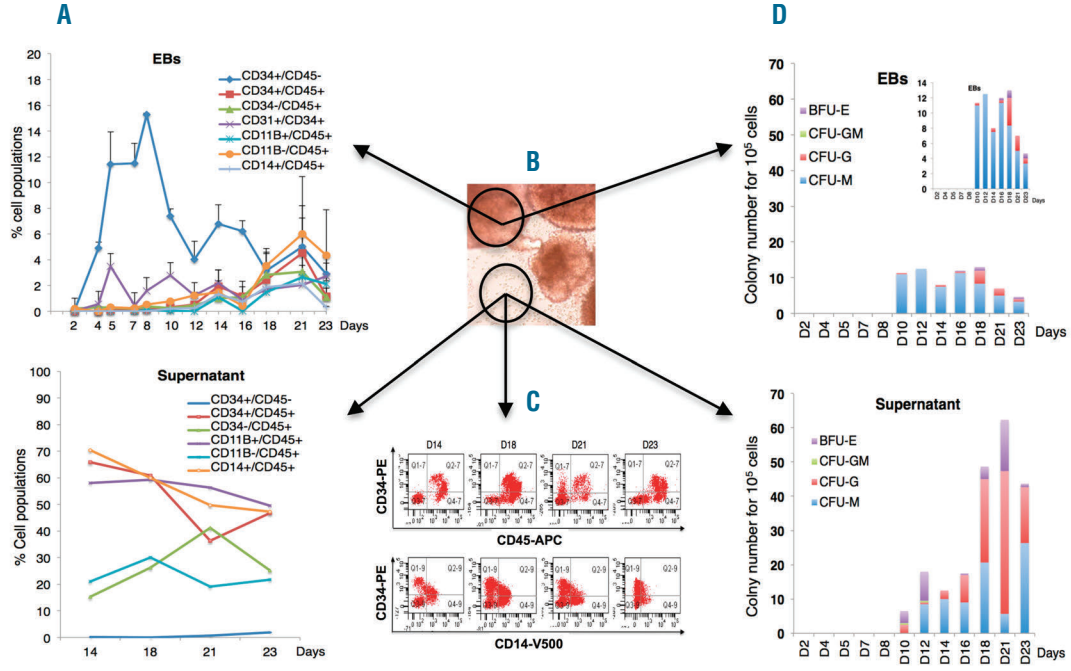

Figure 1. *In vitro* cy-iPSC-cl29 differentiation and hematopoietic cell type characterization. (A) Expression of the NHP hematopoietic markers CD34, CD31, CD45, CD11B and CD14, assessed by flow cytometry on single cells prepared as indicated in B, from EBs (top) or the supernatant (bottom), on days 2, 4, 5, 7, 10, 12, 14, 16, 18, 21 and 23 of differentiation. (B) Typical images of cy-iPSC-derived EBs releasing hematopoietic cells into the supernatant. (C) Representative FACS studies on the supernatant, after 14 days of differentiation. (D) Number of hematopoietic progenitors per 10^5 unsorted EB (top) or supernatant (bottom) cells obtained on the same days as in C. A magnification is shown on the right panel, using a different scale. The data shown are the means of three independent experiments.

forming unit (CFU) assays. On day 14, the CD45$^+$ population accounted for 80% of the cells, 65% of which were CD45$^+$CD34$^+$. The stem/progenitor marker CD34 was gradually lost, with 40 to 45% of cells identified as CD45$^+$CD34$^+$ on day 23. These cells also expressed the monocyte/macrophage markers CD11b and CD14 (Figure 1A-C). In CFU assays, many more hematopoietic colonies developed from supernatants than from EBs cells, which is consistent with cytometry data. Myeloid colonies were the most abundant in both cases, with higher proportions of CFU-M and BFUes in EBs and supernatants, respectively (Figure 1D). We investigated the timing of hemato-endothelial and hematopoietic cell development during cy-iPSC-cl29 differentiation. At around day 5, a population expressing hemato-endothelial markers (CD34$^+$CD31$^+$) and accounting for 2.4% of living cells appeared, together with bipotent hemato-endothelial progenitors (CD34$^+$CD31$^+$CD144$^+$VEGF-R2$^+$CD45-)[7] described as hemogenic precursors.[8] Indeed, 0.3% of cells were CD31$^+$VEGF-R2$^+$, and 80% of these cells were CD144$^+$CD34$^+$. A hematopoietic CD34$^+$CD45$^+$ population first detected on day 10 gradually expanded (*Online Supplementary Figure S3*). We investigated the specific gene expression profiles of EB and supernatant cells at different time points. Expression was compared with that in undifferentiated cy-iPSCs (day 0). On day 2, EB cells strongly expressed *Brachyury* due to BMP4-mediated mesoderm formation. *CDX4*, encoding an upstream regulator of *HOX* genes, was induced on day 2 and repressed after day 7. Expression of *VEGF-R2* and *ERG* peaked on day 4, subsequently decreasing until day 7 and remaining stable thereafter. There were two waves of *GATA-2, SCL/TAL-1*, *Fli-1* and *Tie1* gene expression, the first beginning on day 2 and peaking on day 4 and the second beginning on day 10 and peaking at around day 21. The concomitant expression of the *VEGF-R2, GATA-2, SCL, FLi-1* and *Tie1* genes corroborates the detection of CD144$^+$CD34$^+$CD31$^+$VEGF-R2$^+$ cells at around day 5 and is consistent with efficient differentiation into hemato-endothelial cells, as demonstrated for hESCs.[6,9,10] PU-1 and *RUNX-1* were induced on day 8, with expression peaking on day 18. *CEBPα* expression increased from day 4, peaking on day 21. *GATA-1* was induced after day 15, whereas MYB was not expressed in EB cells (Figure 2A). EB-derived CFU-M and CFU-G activities were correlated with the expression of *PU.1*, *FLi-1* and *CEBPα*, whereas BFU-E erythroid colonies were correlated with the second wave of *SCL, GATA-1*, *FLi-1* and *RUNX-1* expression. Gene expression analysis was also performed on cells recovered from supernatants, but only for days

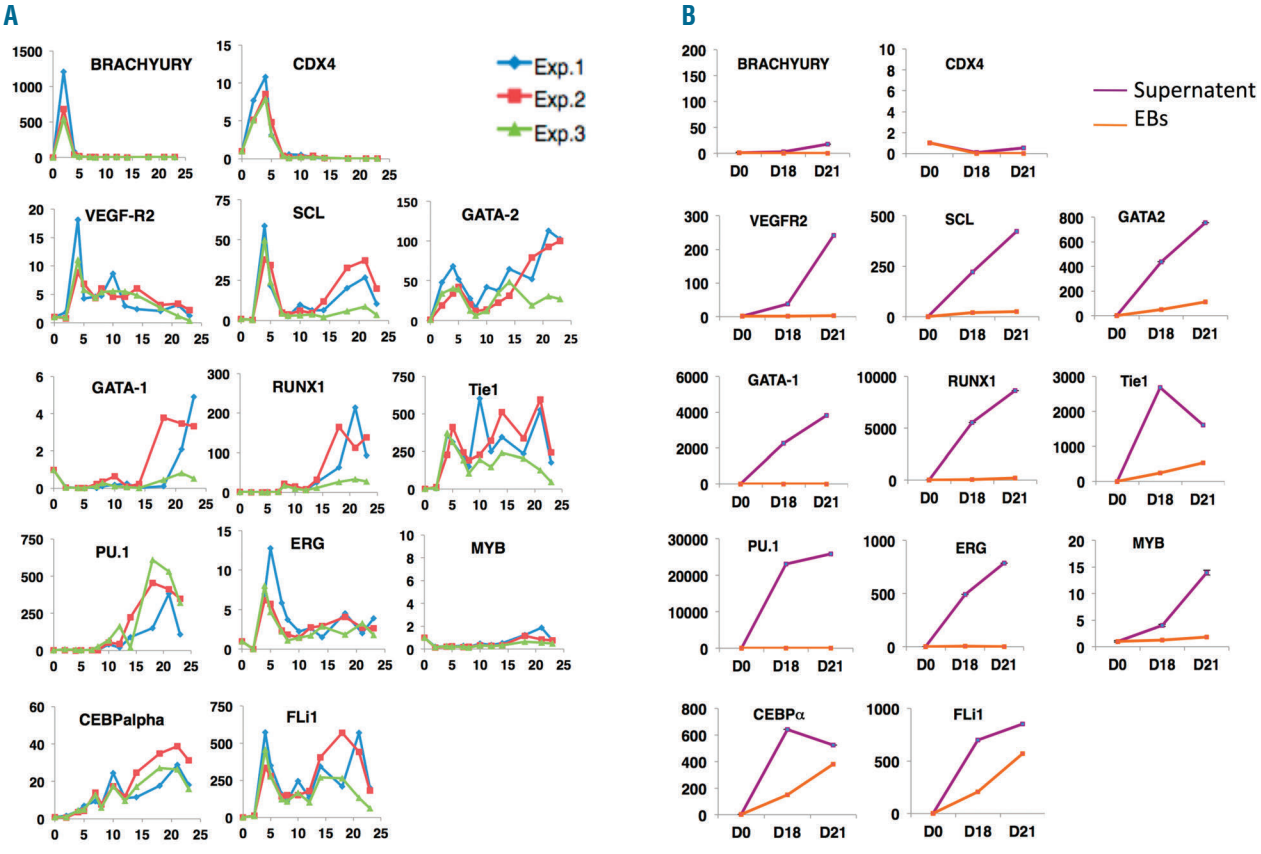

Figure 2. Analysis of gene expression during blood development. (A). Gene expression, analyzed by real-time RT-qPCR, for EB-derived cells on days 2, 4, 5, 7, 10, 12, 14, 18, 21 and 23, with specific *Taq*Man probes for the *Brachyury, CDX4, GATA-2, VEGF-R2, Tie1, SCL, GATA-1, RUNX-1, PU.1, ERG, MYB, CEBPα* and *FLI1* genes. Green, red and blue lines correspond to three independent experiments on cy-iPSC-cl-29. (B). An experiment similar to that shown in A, performed on EB supernatant cells, on days 18 and 21 (purple line). The results are compared with those for EB-derived cells of the same age (orange line). One representative experiment is shown. The numbers on the y axis of A and B indicate the relative fold-change in expression with respect to undifferentiated iPSCs (day 0), after normalization with GAPDH. Different scales are used in A and B.

18 and 21, and compared with those measured in EB cells and undifferentiated (day 0) cells. *Brachyury* and *CDX4* were less strongly expressed than in day 2 EB cells. By contrast, the hemato-endothelial genes *GATA-2, SCL, RUNX-1, MYB, PU-1, CEBP , FLi-1, Tie-1* and *GATA-1* were more strongly expressed than in EB cells (Figure 2B), demonstrating the hematopoietic nature (>90%) of the cells, and confirming FACS and CFU results. Levels of *MYB-1* and *RUNX-1* expression were consistent with a definitive hematopoietic fate[11,12] and the high proportion of CD45$^+$ cells.

We investigated the engraftment potential of cy-iPSC-derived day 17 EB and supernatant cells in NSG mice. We overcame possible homing issues by performing both intrafemoral and retro-orbital injections. 8 of the 10 mice receiving 10^6 unsorted cells (including 10-15% CD34$^+$CD45$^+$ cells) injected into the right femur (RF) displayed up to 0.53% specific NHP-CD45$^+$ cell engraftment in the RF, whereas engraftment of very small numbers of these cells was observed in only three left femurs (LFs), suggesting that cy-iPSC derivatives have a poor homing capacity (Figure 3A,A'). This observation was confirmed by the absence of engraftment in all mice receiving cy-iPSC derivatives by retro-orbital injection (*data not shown*). NHP cells were not detected in mice analyzed 12 weeks after transplantation, indicating that engraftment capacity was transient, as described for mouse and human ES/iPSCs.[13,14] Surprisingly, the intrafemoral injection of an equivalent number of cynomolgus bone marrow (BM) CD34$^+$ cells did not result in higher engraftment rates than for cy-iPSC derivatives in NSG mice, although almost all the RLs and LFs displayed engraftment (Figure 3A). The injection of as few as $5x10^4$ human cord blood CD34$^+$ cells into NSG mice was sufficient to obtain up to 70% engraftment (*data not shown*), suggesting that the weak hematopoietic engraftment observed was specific to monkey-derived cells. In all RFs containing NHP-CD45$^+$ cells from mice receiving hematopoietic cy-iPSC derivatives or Cyno BM CD34$^+$ cells, we detected B-lymphoid (CD45$^+$CD20$^+$), myeloid (CD45$^+$CD14$^+$, CD45$^+$CD11b$^+$) and unidentified hematopoietic cells (CD45$^+$CD20$^-$CD14$^-$CD11b$^-$), but no T-lymphoid cells,

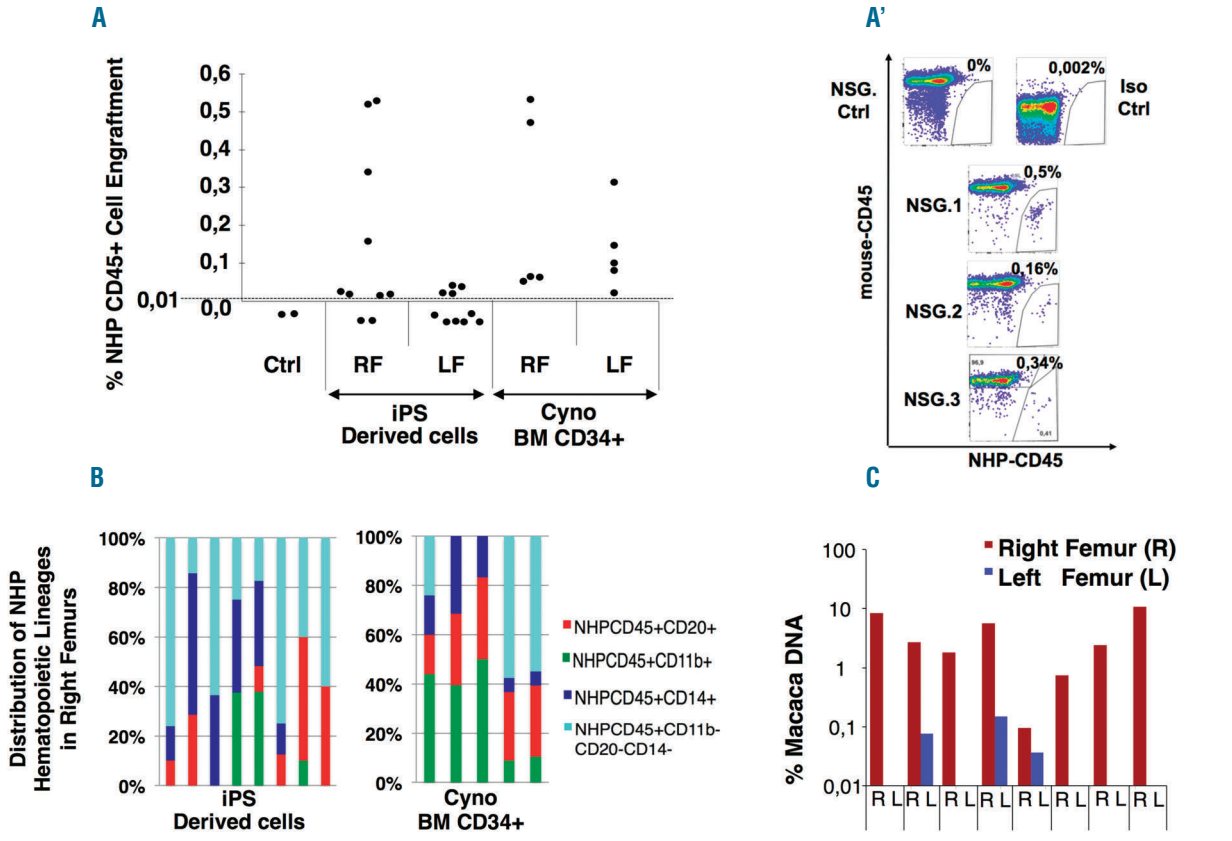

Figure 3. Engraftment of cy-iPSC derivatives in NSG mice. (A) Transplantation of 10^6 unsorted cells obtained from cy-iPSC-derived day-17 EBs, into the right femurs (RFs) of 10 mice. Same number of freshly sorted cynomolgus bone marrow (BM) CD34$^+$ cells transplanted into the RFs of 5 mice. Eight to 10 weeks after transplantation, cells were recovered from the RF and left femur (LF), stained with two specific antibodies against NHP-CD45 and mouse-CD45, and analyzed by flow cytometry. We subjected BM from two untreated mice (Ctrl) to the same antibody staining protocol and determined the threshold (dotted line) for NHP-CD45 positivity, which was set to 0.01%. A flow cytometry image for representative mice is provided in the *Online Supplemental Figure S4*. (A'). Flow cytometry results of 3 representative right femurs of mice engrafted with NHPCD45$^+$mCD45- cells, following transplantation with cy-iPSC-derived day-17 EBs. Cells from untreated mice were subjected to the same antibodies (NSG Ctrl). Isotype control antibodies were also included to determine the amount of background signal (Iso Ctrl). (B). Distribution of cynomolgus myeloid (CD11b$^+$ and CD14$^+$), B-lymphoid (CD20$^+$) and unidentified hematopoietic (CD20$^-$CD14$^-$CD11b$^-$) cells among specific NHP CD45$^+$ cells, as detected in the RFs of mice receiving injections of cy-iPSC derivatives (left panel) or cynomolgus BM CD34$^+$ cells (right panel). Each bar corresponds to one mouse with no specific order of the mice. (C). Proportion of NHP DNA in the total BM DNA retrieved from the right (R) and left (L) femurs of mice receiving injections of cy-iPSC derivatives. We performed qPCR with probes specific for the MIGR vector used for cy-iPSC derivation and mouse actin DNA.

which indicates the absence of definitive HSCs, although they have been shown to be underrepresented in NSG mice[15] (Figure 3B; *Online Supplementary Figure S4*). We confirmed the presence of monkey cells in mice by quantitative PCR and showed that all femurs containing NHP-CD45$^+$ cells, except one LF, tested positive for the specific probe. NHP-DNA accounted for 0.75% to 11% of total mouse BM DNA (Figure 3C). No overall correlation was found between NHP-CD45$^+$ cell percentages and NHP-DNA content in pairwise comparisons (P=0.15). The high levels of NHP-DNA detected suggest that there may also be non-hematopoietic NHP cells (endothelial or mesenchymal) in mouse BM. We were also able to identify Macaca hematopoietic progenitors in mice receiving cy-iPSC derivatives. Cells from two RFs containing NHP-CD45+ cells were plated on methylcellulose and 100 colonies were analyzed by quantitative PCR: 16% and 1% were NHP-specific (*data not shown*).

We show herein that cy-iPSCs can yield hematopoietic engraftment in a cytokine-stimulation protocol. However, the absence of long-term engraftment indicates a lack of definitive HSCs, and highlights the need for an appropriate environment (niche and cytokines) to allow the development and efficient engraftment of these cells. *Macaca nemestrina* iPSCs cocultured on endothelial cells overexpressing JAG1 or DLL4 Notch ligands have recently been shown to generate HSCs with long-term engraftment capacity in immunodeficient mice.[8] It was suggested that a vascular niche expressing JAG1/DLL4 activated Notch signaling in hemangioblastic cells, upregulating the *GATA-2* and *RUNX1* genes, mediating endothelial-to-hematopoietic transition and the emergence of definitive HSCs. In our specific cytokine-induced hematopoietic cells, a hemangioblastic population emerged and hematopoietic genes, including *GATA-2* and *RUNX1*, were activated, consistent with Gori's model; however, short-term engraftment was weaker as compared to their cytokine-induced strategy and there was no long-term engraftment. In the absence of additional modifications, autologous transplantation will undoubtedly provide the most appropriate niche for evaluating the hematopoietic potential of cy-iPSCs.

Soumeya Abed,[1,2,3a] Alisa Tubsuwan,[1,2,4a] Porntip Chaichompoo,[1,2,4] In Hyun Park,[5] Alice Pailleret,[1] Aïssa Benyoucef,[1,6] Lucie Tosca,[7] Edouard De Dreuzy,[1,2,3] Anais Paulard,[9] Marine Granger-Locatelli,[1] Francis Relouzat,[1] Stéphane Prost,[1] Gerard Tachdjian,[7] Suthat Fucharoen,[4] George Q. Daley,[5] Emmanuel Payen,[1,2] Stany Chrétien,[1,2] Philippe Leboulch,[1,8] and Leïla Maouche-Chrétien[1,2]

[1]*CEA, Institute of Emerging Diseases and Innovative Therapies (iMETI), Université Paris Sud 11, France;* [2]*Inserm, Paris, France;* [3]*Université Paris 7, France;* [4]*Thalassemia Research Center, Institute of Molecular Biosciences, Mahidol University, Nakhon Pathom, Department of Biochemistry, Faculty of Medicine Siriraj Hospital and Department of Pathobiology, Faculty of Science, Mahidol University, Bangkok, Thailand;* [5]*Division of Pediatric Hematology/Oncology, Children's Hospital Boston, and Dana-Farber Cancer Institute, Harvard Stem Cell Institute, Harvard Medical School, Boston, MA, USA;* [6]*Inserm U967 - CEA / DSV / IRCM, Fontenay Aux Roses Cedex, France;* [7]*Hôpital Antoine Béclère, Service d'Histologie Embryologie Cytogénétique,"Assistance Publique - Hôpitaux de Paris", Clamart, France;* [8]*Genetics Division, Department of Medicine, Brigham & Women's Hospital and Harvard Medical School, Boston, MA, USA and* [9]*Bluebirdbio, Cambridge, MA, USA*

[a]*These authors contributed equally to this work.*

Acknowledgments: we thank B. Gillet-Legrand (Bluebird bio), S. Guenounou, A. Cosma and J. Baijer (CEA, Fontenay aux Roses) and D. Pineau (Béclère Hospital) for excellent technical contributions. We thank F. Pflumio for providing advice for mouse experiments.

Funding: this work was supported by INSERM, Chaire industrielle de l'Agence Nationale pour la Recherche (ANR) to P.L. and a Liv-iPS ANR grant for the monkey iPSC project awarded to P.L and L.MC. S.A. was supported by the French Research Ministry and the French Society of Hematology (SFH), A.T was supported by a fellowship from Mahidol University and an RGJ-PHD scholarship from the Thailand Research Fund. PC was supported by a Junior Research Fellowship from the French Embassy in Thailand. E.DD. was supported by a CEA IRTELIS scholarship, France.

Correspondence: leila.maouche@inserm.fr
doi:10.3324/haematol.2015.127373

Key words: Nonhuman primate, Induced pluripotent stem cells, Engraftment of cy-iPSC-derived hematopoietic cells

Information on authorship, contributions, and financial & other disclosures was provided by the authors and is available with the online version of this article at www.haematologica.org.

References

1. Park IH, Lerou PH, Zhao R, Huo H, Daley GQ. Generation of human-induced pluripotent stem cells. Nat Protoc. 2008;3(7):1180-1186.
2. Huangfu D, Osafune K, Maehr R, et al. Induction of pluripotent stem cells from primary human fibroblasts with only Oct4 and Sox2. Nat Biotechnol. 2008;26(11):1269-1275.
3. Okano M, Bell DW, Haber DA, Li E. DNA methyltransferases Dnmt3a and Dnmt3b are essential for de novo methylation and mammalian development. Cell. 1999;99(3):247-257.
4. Okahara-Narita J, Umeda R, Nakamura S, Mori T, Noce T, Torii R. Induction of pluripotent stem cells from fetal and adult cynomolgus monkey fibroblasts using four human transcription factors. Primates. 2012;53(2):205-213.
5. Schlesinger S, Goff SP. Silencing of proviruses in embryonic cells: efficiency, stability and chromatin modifications. EMBO Rep. 2013;14(1):73-79.
6. Wang L, Li L, Shojaei F, et al. Endothelial and hematopoietic cell fate of human embryonic stem cells originates from primitive endothelium with hemangioblastic properties. Immunity. 2004;21(1):31-41.
7. Ayllon V, Bueno C, Ramos-Mejia V, et al. The Notch ligand DLL4 specifically marks human hematoendothelial progenitors and regulates their hematopoietic fate. Leukemia. 2015;
8. Gori JL, Butler JM, Chan YY, et al. Vascular niche promotes hematopoietic multipotent progenitor formation from pluripotent stem cells. J Clin Invest. 2015;125(3):1243-1254.
9. Narula J, Smith AM, Gottgens B, Igoshin OA. Modeling reveals bistability and low-pass filtering in the network module determining blood stem cell fate. PLoS Comput Biol. 2010;6(5):e1000771.
10. Gottgens B, Nastos A, Kinston S, et al. Establishing the transcriptional programme for blood: the SCL stem cell enhancer is regulated by a multiprotein complex containing Ets and GATA factors. EMBO J. 2002;21(12):3039-3050.
11. Samokhvalov IM, Samokhvalova NI, Nishikawa S. Cell tracing shows the contribution of the yolk sac to adult haematopoiesis. Nature. 2007;446(7139):1056-1061.
12. Ueno H, Weissman IL. Stem cells: blood lines from embryo to adult. Nature. 2007;446(7139):996-997.
13. Tubsuwan A, Abed S, Deichmann A, et al. Parallel assessment of globin lentiviral transfer in induced pluripotent stem cells and adult hematopoietic stem cells derived from the same transplanted beta-thalassemia patient. Stem Cells. 2013;31(9):1785-1794.
14. Ledran MH, Krassowska A, Armstrong L, et al. Efficient hematopoietic differentiation of human embryonic stem cells on stromal cells derived from hematopoietic niches. Cell Stem Cell. 2008;3(1):85-98.
15. McDermott SP, Eppert K, Lechman ER, Doedens M, Dick JE. Comparison of human cord blood engraftment between immunocompromised mouse strains. Blood. 2010;116(2):193-200.